# *Botrytis cinerea* small RNAs are associated with tomato AGO1 and silence tomato target genes supporting cross-kingdom RNAi between the fungal pathogen *B. cinerea* and its tomato host

Baoye He[1,#], Qiang Cai[2,#], Arne Weiberg[3,#,*], An-Po Cheng[3], Shouqiang Ouyang[4], Katherine Borkovich[1], Jason Stajich[1], Cei Abreu-Goodger[5], Hailing Jin[1,*]

[1]Department of Microbiology and Plant Pathology, Center for Plant Cell Biology, Institute for Integrative Genome Biology, University of California, Riverside, CA, USA.

[2]State Key Laboratory of Hybrid Rice, College of Life Science, Wuhan University, Wuhan, China.

[3]Faculty of Biology, Genetics, LMU Munich, Martinsried, Germany.

[4]Joint International Research Laboratory of Agriculture and Agri-Product Safety of Ministry of Education of China, Yangzhou University, Yangzhou JS, China.

[5]Institute of Ecology and Evolution, School of Biological Sciences, The University of Edinburgh, Edinburgh EH9 3FL, United Kingdom

# Contribute equally
*Corresponding authors
hailingj@ucr.edu, A.Weiberg@biologie.uni-muenchen.de

**Abstract**

Cross-kingdom or cross-species RNA interference (RNAi) is broadly present in many interacting systems between microbes/parasites and their plant and animal hosts. Recent study by Qin *et al.* (2022) performed correlation analysis using global sRNA- and mRNA-deep sequencing data of cultured *B. cinerea* and *B. cinerea*-infected tomato leaves and claimed that cross-kingdom RNAi may not occur in *B. cinerea*–tomato interaction (Qin *et al.*, 2022). In this response letter, we use experimental evidence and additional bioinformatics analysis of the datasets produced by Qin *et al.* (2022) to identify the key reasons why a discrepancy with previously published findings occurred. Here, we also provided additional experimental evidence to support the presence of cross-kingdom RNAi between tomato and *B. cinerea.* We believe it is important to clarify the basic concept and mechanism of cross-kingdom/cross-species sRNA trafficking and illustrate proper bioinformatics analyses in this regard for all the scientists and researchers in this field.

Cross-kingdom or cross-species RNA interference (RNAi) is a phenomenon in which small RNAs (sRNAs) are transported between interacting organisms to silence the expression of target genes in the adversary or interacting partner (Weiberg *et al.*, 2013, Cai *et al.*, 2018, Weiberg *et al.*, 2014). Our lab first discovered this communication mechanism between plants and the fungal pathogen *Botrytis cinerea*. Some sRNAs of *B. cinerea* are transported into host plants where they hijack host RNAi machinery for cross-kingdom gene silencing (Weiberg et al., 2013). We found that the transferred fungal sRNAs are loaded into the host Arabidopsis Argonaute 1 (AGO1) protein to silence host target genes involved in immune responses (Weiberg et al., 2013). This phenomenon has since been observed later in many different interacting organisms. For example, other plant fungal pathogens (such as *Fusarium oxysporum, Verticillium dahliae*), oomycete pathogens (such as *Hyaloperonospora arabidopsidis*), the parasitic plant *Cuscuta campestris*, and even the symbiotic ectomycorrhizal fungus *Pisolithus microcarpus* and the bacterial symbiont Rhizobium (*Bradyrhizobium japonicum*) can send a set of sRNAs into the host plant to silence the expression of host target genes (Dunker *et al.*, 2020, Shahid *et al.*, 2018, Ren *et al.*, 2019, Wong-Bajracharya *et al.*, 2022, Ji *et al.*, 2021, Zhang *et al.*, 2022). Furthermore, the mode of action of transferred microbial sRNAs seems also to be conserved. The sRNAs from *F. oxysporum* (Ji et al., 2021)*, V. dahliae* (Wang et al., 2016), *H. arabidopsidis* (Dunker et al., 2020) and the *Rhizobium* (Ren et al., 2019) also utilize host AGO proteins for silencing host target genes. Excitingly, cross-kingdom or cross-species RNAi has also been observed in animal-pathogen or parasite interaction systems. For example, the fungal pathogen of mosquito, *Beauveria bassiana* transfers a microRNA-like RNA (milRNA) to the host cells. This milRNA is loaded into mosquito AGO1 to silence the host immunity gene *Toll receptor ligand Spätzle 4* (Cui *et al.*, 2019). Some parasites, such as the gastrointestinal nematode *Heligmosomoides*. *Polygyrus,* send a range of its sRNAs into mammalian gut cells to target and silence immunity and inflammation-related genes (Buck *et al.*, 2014, Chow *et al.*, 2019). The causal bacterial pathogen for human Legionnaires' disease, *Legionella pneumophila* also sends bacterial sRNAs into human host cells to regulate the expression of innate immune response genes (Sahr *et al.*, 2022). Thus, cross-kingdom/cross-species RNAi is widely observed and accepted by scientists studying many interaction systems between microbes/pests and their plant or animal hosts.

Recently, Qin *et al.* (2022) performed sRNA- and mRNA-deep sequencing analysis of cultured *B. cinerea* and *B. cinerea*-infected tomato leaves and claimed that cross-kingdom RNAi does not occur in *B. cinerea*–tomato interaction (Qin *et al.*, 2022). Based on their results, they also criticized multiple previously published papers on cross-kingdom RNAi, including a couple from our lab. In this response letter, we address the questions raised in this study. This response is not intended to dismiss the argument of Qin and colleagues but to use experimental evidence and additional bioinformatics analysis of the datasets produced by Qin *et al.* (2022) to identify the key reasons why a discrepancy with previously published findings occurred. Here, we also provided additional experimental evidence to support the presence of cross-kingdom RNAi between tomato and *B. cinerea.* We believe it is important to clarify the basic concept and mechanism of cross-kingdom/cross-species sRNA trafficking and to illustrate proper bioinformatics analyses in this regard for all the scientists and researchers in this field.

**1. The assumptions underlying the bioinformatics analysis by Qin *et al*. (2022) are flawed for cross-kingdom RNAi.**

Qin *et al.* (2022) performed a correlative analysis of sRNA and mRNA transcriptome profiling to find evidence for cross-kingdom RNAi in the *B. cinerea*-tomato interaction. They identified a total of 27,918 unique *B. cinerea* sRNAs with sizes of 20-24nt from *B. cinerea*-infected tomato leaves harvested at 12, 16, and 24 h post-infection (hpi) as well as from *B. cinerea* grown in liquid culture. They used the entire 27,918 sRNA set, including 70-90% sRNAs derived from *B. cinerea* ribosomal RNAs (rRNAs) and transfer RNAs (tRNAs), to perform target prediction analysis in the tomato genome. Among them, 7,042 *B. cinerea* sRNAs were predicted to target 3,185 distinct tomato mRNAs. Conversely, 114,011 tomato sRNAs were found that were predicted to target 11,434 *B. cinerea* mRNAs. Based on the sRNA-seq and mRNA-seq data, the authors observed a weak negative correlation between the entire set of sRNAs and their potential targets that was not significant according to a permutation analysis. Thus, they concluded that there was no evidence for cross-kingdom RNAi in the *B. cinerea*-tomato interaction. This conclusion is based on the assumptions that all sequenced *B. cinerea* sRNAs can contribute to cross-kingdom RNAi, that an important part of the plant gene expression changes observable by mRNA-seq are caused by fungal sRNAs, and that predictions

of sRNA-mRNA interactions have low levels of false positives. We believe that these assumptions are flawed for the following reasons:

1) Not all sequenced sRNAs of *B. cinerea* are genuine extracellular sRNAs, not all extracellular sRNAs would translocate into the host cells, and not all sRNAs that do enter host cells will form a functional silencing complex, e.g. with the host AGOs. Even within the same organism, not all sRNAs can silence their bona fide targets at any given time. Many sRNAs, such as most mammalian miRNAs, can have an average of 300-400 predicted targets, and some even have over 1000 predicted target genes. However, many studies have shown that only a small subset of these target genes' transcripts are reduced in abundance at any given time under specific developmental stages or in response to various environmental cues, whereas the majority of the predicted target genes are not suppressed (Bartel, 2009, Wilczynska & Bushell, 2015). This phenomenon cannot lead to a conclusion that there is no evidence for mammalian miRNA to induce silencing of target genes. Thus, global sRNA-mRNA correlation analysis for cross-kingdom/cross-species RNAi is meaningless.

2) The quality and reproducibility of Qin *et al.*'s sRNA- and mRNA-seq datasets are low (see below for details). The sRNA data in particular includes large amounts of reads mapping to rRNA and tRNA (up to over 90%) for all their analysis (Figure 2B-D). This could be an indication of low-quality and highly degraded RNA, and these sequences will mask any real silencing patterns. Restricting the analysis to sRNAs of 20-24nt, as per Qin *et al.*'s methods, will help increase the signal-to-noise ratio, as would excluding some reads mapping to rRNA/tRNA. Nevertheless, these steps will not effectively remove the problem, since all the RNA in these samples would have suffered similar levels of degradation, and even 20-24nt reads would include a large fraction of irrelevant degradation products. In fact, according to Figure 2 in Qin *et al.* 49% of the selected unique sRNA sequences map to rRNA or tRNA loci.

3) Qin *et al.* predicted tomato targets by using the psRNATarget tool with the default settings of V2 2017, without any further requirements. These settings allow bulges and gaps in the target site base pairing and up to two mismatches in the seed region. An Expectation score of 5 was used as a cut-off. The stringency of these settings for plant target prediction is rather low, because gene silencing rarely occurs with a bulge or gap in the sRNA-target pairing regions and mismatch at the $10^{th}$ -$11^{th}$ nt positions will block the function of sRNA, which was the principal basis for designing the short tandem target mimic (STTM) to block the function of sRNAs (Yan

*et al.*, 2012). To achieve more precise target prediction, in our previous paper (Weiberg et al., 2013), we used the TAPIR1.1 tool to predict tomato targets with more stringent requirements: a) No gap or bulge within the alignment between the sRNA and the target was allowed; b) The 10$^{th}$ and 11$^{th}$ nts of the sRNA must perfectly match its target; c) At most one mismatch or two wobbles were allowed from position 2 to 12; d) A maximum of two continuous mismatches was allowed; e) A score of 4.5 was used as a cutoff.

Thus, the extremely high number of tomato target genes predicted by Qin *et al.* (2022) was most likely overestimated and thus many of their predicted target genes in tomato may not be true Bc-sRNA targets. Importantly, even true sRNA/mRNA targets will not be functional unless at the very least they are present in the same cell and within a silencing complex.

Most importantly, we believe that the essential step after the deep-sequencing and bioinformatics analyses is to perform experimental validation analysis, preferably using multiple different approaches, to confirm all the conclusions drawn from any omics analysis. All the studies from our labs have followed this principle and we always use molecular, biochemical, cell biological and/or genetics approaches to confirm any results we obtained from omics data.

## 2. Some *B. cinerea* sRNAs associate with tomato AGO1 supporting the presence of cross-kingdom RNAi between *B. cinerea* and tomato.

We previously observed that a subset of *B. cinerea* sRNAs move into plant cells and utilize *Arabidopsis* AGO1 proteins to silence host target genes (Weiberg et al., 2013). Following *Arabidopsis* AGO1 co-immunopurification and RNA isolation, the *B. cinerea* Bc-siR3.1, Bc-siR3.2 and Bc-siR5 were detected by a stem-loop RT-PCR method. The same molecular mechanism was also found in plant pathogens *F. oxysporum, V. dahliae*, *H. arabidopsidis*, animal fungal pathogen *Beauveria bassiana* and even in beneficial bacterial symbiont *Rhizobium* during cross-kingdom RNAi with their hosts (Ji et al., 2021, Zhang et al., 2022, Dunker et al., 2020, Ren et al., 2019). The sRNAs from these microbes are loaded into host AGO proteins to silence host target genes.

In order to experimentally validate whether cross-kingdom RNAi is present between *B. cinerea*-tomato during infection, the most straightforward way is to examine whether any *B. cinerea* sRNAs are associated with tomato AGO proteins after moving into tomato cells by performing tomato AGO1-immunoprecipitation (AGO1-IP) analysis. We utilized the tomato

AGO1 antibody generated by the Katherine Borkovich lab, which was used to successfully pull down tomato sRNAs (Ji et al., 2021), and immunoprecipitated the sRNAs associated with the tomato AGO1 after *B. cinerea* infection.

We indeed detected some incorporated Bc-sRNAs. The three Bc-sRNAs described in our previous study (Weiberg et al., 2013) and also detected in Qin et al. (2022), Bc-siR3.1, Bc-siR 3.2, and Bc-siR5, were detected to be associated with tomato AGO1 complex at 12, 16 and 24 hpi (Figure 1A). We also checked Bc-sRNAs predicted to target tomato genes by Qin *et al.*(2022) and mapped them to annotated regions in the *B. cinerea* B05.10 genome. We found that two of the Bc-sRNAs (#3 and #5) were also associated with tomato AGO1 (Figure 1B). As expected, the transcript accumulation of their predicted tomato target genes was reduced during the infection (Figure 1C), supporting that Bc-sRNA-mediated silencing of target genes occurred in tomato. At least one of the Bc-sRNA#3 tomato targets, *SISKP2,* was down-regulated after infection (Figure 1C). Silencing of a Bc-sRNA#5 target *SIRLK* was also detected by Qin *et al.* in Figure 4 of Qin *et al.* (2022). Thus, we demonstrated that cross-kingdom RNAi is evident between *B. cinerea* and tomato. However, many Bc-sRNAs identified by Qin *et al.* (2022) were not associated with tomato AGO1 (#4,#6,#8,#9 in Figure 1B), which could explain why they did not silence the expression of corresponding predicted targets in tomato (Figure 1C).

**3. Many sRNA- and mRNA-seq libraries of the Qin *et al.*(2022) study were not deposited in NCBI, and among the deposited datasets, the correlation efficiencies between the biological replicates and the quality of the sequencing datasets were still quite low.**

To fully understand the results and conclusions from Qin *et al.* (2022), we decided to reanalyze their deep-sequencing data. In order to avoid the appearance of potential bias, we also invited another two independent hard-core bioinformatics groups (Jason Stajich and Cei Abreu-Goodger), both of whom have extensive experience in sRNA-seq analysis, to reanalyze Qin *et al.* 's sRNA-seq and mRNA-seq datasets. All three groups obtained similar results and reached to the same conclusion: the overall reproducibility and the quality of Qin *et al.*'s deep sequencing data are low, and several analyses had some obvious flaws, which we detailed below.

First, it's surprising that many sRNA- and mRNA-seq datasets produced by Qin *et al.* were not deposited in NCBI (SRP166089). Qin *et al.* (2022) claimed to use four biological replicates for each data point (shown in Qin *et al.*'s Table S1), but only two or three biological replicates

for each data point were selected to be deposited into the NCBI database (SRP166089). For example, 22 different sRNA libraries were described in their supplemental tables, yet only 13 libraries, including only one for each of the mock samples, were available for download (Table 1). In addition, 24 different mRNA libraries were analyzed in *Qin* et al.; but only 17 libraries were available for download (Table 2). Critically, the entire datasets for *ku70* mutant and the *dcl1dcl2* double mutant generated in the *ku70* background are completely missing, although these were one of the most important datasets that their conclusions were based on.

Second, to assess the reproducibility and the quality of Qin *et al.*'s sRNA-seq dataset, we performed principal component analysis (PCA) and sRNA mapping distribution analysis. As shown in Figure 2A, the reproducibility among the biological repeats is low. Figure 2B shows two examples of the sRNA size and mapping distribution of the two biological repeats of cultured *B. cinerea* (upper panel, B16As and B16Bs) and the three biological repeats of the infected tomato sample collected at 12 hpi (Lower panel I12As, I12Bs, I12Cs). The size and mapping distribution between the replicates are very different. For example, the first replicate of cultured *B. cinerea* (B16_1) shows a relatively uniform sRNA size distribution across 18-38 nt, with no obvious peak around 20-24nt. This is a typical pattern for degraded RNA, which is corroborated by the high levels of rRNA and tRNA-mapping reads. The second cultured *B. cinerea* replicate (B16_2), as well as the first two replicates of infected tomato samples (I12_1 and I12_2), show a main peak at 33 nt, mainly consisting of tRNA fragments., while the third replicate (I12_3) shows an substantially different profile (Figure 2B). If we assume that TE-derived sRNAs are likely to be responsible for cross-kingdom RNAi, the proportion of such reads varies drastically between the sequenced. In general, we found that the vast majority of *B. cinerea* sRNAs claimed in Qin *et al.*'s dataset are derived from the sense strand of rRNAs and tRNAs (Figure 2C). For example, over 90% of the sRNAs from both cultured *Botrytis* libraries are from sense strands of rRNAs and tRNAs. Independently, we further analyzed the sRNAs mapped to the protein-coding regions (Figure 2D). Again, most of the sRNA reads are derived from the sense strand of the RNAs. This is another indication that these sRNA detected are most likely degradation products.

Third, we also performed PCA analysis to assess the reproducibility of the Qin *et al.* (2022) mRNA-seq dataset. Similarly, the biological repeats are not grouped according to the general biological expectation (Figure 3A). Two of the 16h infected libraries and one of the 12h infected

library were grouped with one 12h mock and 16h mock libraries, and two 24h mock libraries grouped with three 24h infection libraries (Figure 3A), indicating that the mRNA sequencing data have low repeatability and quality. To determine if the difference within each group is statistically significant, we performed differential expression analyses between infected and mock samples at each time point, and visualized results using volcano plots based on the FDR (false discovery rate) and foldchange value between different replicates and treatments. When using an FDR <0.05 and |log2foldchange>1| were used as a cutoff, there are few (43 mRNAs) and no mRNAs with significant changes in "Infection 12 hours" and "Infection 24 hours," respectively (Fig. 3B-3D). Thus, using these data to determine the expression levels of Bc-sRNAs targeted mRNAs is most likely inaccurate.

**4. Misinterpretation of sRNA production by the *ms3003* element**

Qin *et al*. (2022) decided to generate *ms3003* deletion mutant strains because "approximately 10% of the total sRNAs produced by *B. cinerea* strain B05.10 originated from a retrotransposon region on Chr14 annotated as *ms3003*". Several misleading interpretations were made here:

First, estimating sRNA production per retrotransposon (RT) locus based on total sRNA read counts makes no sense because many sRNAs map multiple times and to different RT loci, leading to a doubling of sRNA read counts. Without knowing which element(s) is/are true sRNA-producing locus/i, the counts should be at least divided by the number of mapping events for estimation. Therefore, the 10% mentioned above of sRNA reads derived from the *ms3003* locus is misleading.

Second, there are even more fragmented RT elements (loci) - we have previously identified additional 221 RT loci of > 400 bp fragments (Porquier *et al.*, 2021)- dispersed over the *B. cinerea* genome, that have not been considered as source of sRNA production by Qin *et al*., and which are making a valid estimation of the relative sRNA production per individual RT element/locus extremely complicated (if not impossible).

Third, it is not indicated by Qin *et al*. (2022), which sRNA library was used for estimating the percentage of sRNAs produced per RT element (as given in Fig.S3). This is highly relevant because we recently found that sRNAs mapping to different RTs, in particular belonging to the *Bc*Gypsy3 family, are highly up-regulated during tomato infection (Porquier et al., 2021) .

There are contradictory results and interpretations in Qin *et al*. (2022). Deleting the *ms3003* element certainly did not certainly lead to a drastic loss of sRNA production, as suggested by Qin *et al*. (2022). In fact, their own data supports the continuous production of RT-derived sRNAs, as shown in Fig.5c of Qin *et al*. In order to make any statement about altered sRNA production, the authors should provide sRNA sequencing data for the *ms3003* mutants.

**5. Qin *et al.* (2022) used a non-representative infection assay with an unusually high spore concentration that masked the phenotype of reduced virulence of their Δ*bcdcl1*/Δ*bcdcl2*/*ku70* mutant strains.**

Qin *et al*. argue that their Δ*bcdcl1*/Δ*bcdcl2* mutant generated in the *ku70* mutant background did not exhibit any reduction of virulence on tomato leaves and other tested plant species. For this experiment, they used an unusually high spore concentration of 1000 conidia/µl suspended in potato dextrose broth (PDB), a rich culture medium that allows rapid growth of *B. cinerea* in vitro, to inoculate the detached leaves. It is worth noting that tomato is a better host for *B. cinerea* than Arabidopsis.

We have now repeated infection assays with detached tomato leaves using 10 µl of 10 conidia/µl spore concentrations, resuspended in 1% malt extract. We think this lower spore concentration better represents the natural infection pressure. Under this infection condition, we observed significantly reduced lesion formation in two independent *ku70* Δ*bcdcl1*/Δ*bcdcl2* mutant strains at 60 hours post-inoculation (Figure 4).

We would like to point out that the involvement of DCLs in fungal virulence was also observed in other fungal species and by other laboratories. Several studies reported that *dcl* deletion in fungal pathogens compromises infection, for example, in *Fusarium graminearum, Penicillium italicum, Colletotrichum gloeosporioides* and *Valsa mali* (Wang *et al.*, 2017, Werner *et al.*, 2021, Yin *et al.*, 2020, Feng *et al.*, 2017).

**6. Qin *et al.* used an inappropriate NHEJ DNA repair mutant *ku70* to generate Δ*Bcdcl1*/Δ*Bcdcl2* mutants using the CRISPR/CAS9 system.**

Qin *et al*. claimed that they generated Δ*Bcdcl1*/Δ*Bcdcl2* mutant strains using the Cas9 RNP strategy (Leisen *et al.*, 2022) in a *B. cinerea* B05.10 *ku70* mutant background. This *B. cinerea ku70* mutant strain is compromised in a non-homologous end-joining DNA repair

(NHEJ) system and favors homologous recombination to gain targeted gene knock-out (Choquer *et al.*, 2008, Pinedo *et al.*, 2008). However, we think that double deletion of NHEJ and *DCL*s genes should be considered with caution for two reasons:

First, a *ku70* mutant in the fungus *Penicillium digitatum* is affected in growth and conidia production (Gandía *et al.*, 2016), which means that pleiotropic effects may occur due to increased sensitivity to DNA damage. In addition, RNAi mutants including *dcl*s showed increased sensitivity to DNA damage in *Neurospora crassa (Lee et al., 2009)*, a phenomenon that is well-studied in the mammalian field as well (Tang & Ren, 2012, Bonath *et al.*, 2018, Lu *et al.*, 2018). Therefore, NHEJ plus DCLs deletion might likely cause unpredictable complications in terms of DNA repair and genome integrity.

Second, it might also be a problem when combining *ku70* mutant with CRISPR CAS9 system. CAS9 is known to generate unpredicted off-target cleavages, which largely rely on NHEJ DNA repair system. The combination of CAS9 and *ku70* mutation can also generate more unpredicted mutation sites in the background. Many people in the field of mammalian and plant fungal pathogens are always hesitant in using *ku70/ku80* mutants because they are fully aware that knockout NHEJ DNA repair function may cause many unpredicted mutations in the genome and also make the organisms more sensitive to DNA damage.

**7. Qin *et al.* (2022) statement "Deleting *B. cinerea Bcdcl1* and *Bcdcl2* eliminated transposon-derived sRNAs, but did not affect virulence" is incorrect.**

Qin *et al*. (2022) stated that "transposon-associated sRNAs are eliminated in the Δ*bcdcl1/*Δ*bcdcl2"*, according to their sRNA-seq data. To confirm their statement, we would have to re-analyze the sRNA-seq datasets of *B. cinerea ku70* and Δ*bcdcl1/*Δ*bcdcl2*. However, in contrast to the open research statement in Qin *et al.* (2022), these raw sequencing data are not available in the NCBI repository under the given project number SRP166089.

We instead designed PCR primers to detect nine sRNAs, as analyzed by Qin *et al*. (2022) in their Fig.4 and Fig.S1, via stem-loop RT-PCR (Varkonyi-Gasic *et al.*, 2007a). We detected nine out of nine sRNAs in the B05.10 WT and *ku70* mutant strain and eight out of nine in two independent Δ*bcdcl1/*Δ*bcdcl2/ ku70* strains (Figure 5). After mapping these nine sRNA candidates to annotated regions in the *B. cinerea* B05.10 genome (Figure 1B), we found only four sRNAs mapped to retrotransposons with one sRNA mapped to both a retrotransposon and

an exon (Bcin16g04520) locus. Thus, many RT-derived sRNAs are still present in the Δ*bcdcl1/*Δ*bcdcl2/ku70* mutants. Deleting *B. cinerea Bcdcl1* and *Bcdcl*2 cannot eliminate all transposon-derived sRNAs. Furthermore, our Δ*bcdcl1/*Δ*bcdcl2* double mutant is different from the Δ*bcdcl1/*Δ*bcdcl2/ku70* triple mutant that Qin *et al.* generated. Some *Botrytis* sRNAs, for example, Bc-sRNA#3 is still present in Δ*bcdcl1/*Δ*bcdcl2/ku70* mutant but not in our Δ*bcdcl1/*Δ*bcdcl2* mutant (Figure 5). This sRNA can associate with tomato AGO1 protein to suppress the target gene expression, which strongly supports that these different *dcl* double mutants have different sRNA patterns and finally effect their virulence.

In summary, all the new experimental evidence presented here demonstrates that Qin *et al.*'s conclusion that cross-kingdom RNAi does not occur between *B. cinerea* and tomato is not supported by reliable experimental evidence or correct interpretation of existing data.

**Figure legends**

**Figure 1. Detecting Bc-sRNAs by tomato AGO1 immunoprecipitation and tomato target gene expression during the infection.** (A) and (B) Bc-sRNAs from our previous study (A) and from the Qin *et al.*(2022) study (B) were detected after tomato AGO1-IP, followed by RT-PCR. (C) Tomato target gene expression was detected using real-time PCR. RT, retrotransposons; UTR, untranslated region.

**Figure 2**. The reproducibility and quality of Qin *et al.* (2022) sRNA datasets are low. (A) Principal component analysis (PCA) of 10 *Botrytis* sRNA libraries. Please note there was only one library for each of the three mock treatments available. We did not used them for PCA analysis. (B) Genomic origin and size distribution of sRNAs from two *Botrytis* culture samples and three infected tomato plant replicates, which show very different patterns among biological replicates. (C) The distribution of reads from Qin *et al.*(2022) sRNA libraries that map to the different parts of the *Botrytis* genome. (D) The distribution of reads from Qin *et al.*(2022) sRNA libraries that map to coding regions (D). Coding of samples: I= inoculated tomato leaves; M=mock-treated tomato leaves; B= *B. cinerea* liquid culture; 12, 16, 24 = time point of sampling after inoculation (hours); A, B, C, D = biological replicate sample that was sequenced by Qin *et al.*(2022); s=sRNA fraction.

**Figure 3. The reproducibility and quality of Qin *et al.* (2022) mRNA datasets are low.** (A) Principal component analysis (PCA) of mRNA libraries. (B-D) Volcano plot of differentially expressed genes (DEGs). The expression difference is significant for FDR <0.05 and |log2foldchange>1|. Coding of samples: I= inoculated tomato leaves; M=mock-treated tomato leaves; B= *B. cinerea* liquid culture; 12, 16, 24 = time point of sampling after inoculation (hours); A, B, C, D = biological replicate sample that was sequenced by Qin *et al.*; m= mRNA fraction.

**Figure 4: Infection assay of Δ*bcdcl1*/Δ*bcdcl2*/*ku70* on detached tomato leaves.** Inoculation was performed with 100 conidiospores per inoculation, and lesion areas were analyzed at 60 hours post-inoculation (hpi). At least 30 lesions were measured per strain and condition, and

inoculation assays were repeated three times with similar results. Letters indicate significant differences when using one-way ANOVA and Tukey test with $p<0.05$.

**Figure 5: the Δ*bcdcl1*/Δ*bcdcl2* mutants produce sRNAs.** Production of 9 BcsRNAs was tested in different *B. cinerea* genotypes by stem-loop RT-PCR.

## Materials and methods

### *Botrytis* and plant growth

The *B. cinerea* (Pers.: Fr.) strain B05.10, *ku70* mutant, and all three Δ*bcdcl1*/Δ*bcdcl2* mutant strains were cultured on HA medium (4 g/L yeast extract, 4 g/L glucose, 10 g/L malt extract 15 g/L agar) for leaf inoculation assay. The plates were incubated for 2 weeks at room temperature under the exposure of UV-Tube Complete Set, metal, 18W/60 cm (Eurolite®) to stimulate sporulation. Liquid-cultured *Botrytis* was used for RNA extraction and stem-loop PCR. $2x10^5$ conidia were cultured in 50 ml HA liquid medium at 22 °C for 20 h.

Tomato *S. lycopersicum* (L.) Heinz cultivar was used as a plant host in this study. Tomato seeds were incubated in a petri dish half-filled with sterile water in darkness at 22 °C for 3 days. Then the seeds were transferred into soil and grew for 5-6 weeks at 22 °C with 60% humidity and with 16 h/8 h light/darkness.

### Tomato AGO1 immunoprecipitation (IP)

Tomato AGO1 antibody from Dr. Borkovich's lab was used to pull down the sRNAs associated with the AGO1 protein(Ji et al., 2021). Tomato AGO1 IP was performed with 5 g fresh leaves collected at 0, 12, 16 and 24 h after spray inoculation with *B. cinerea*. Tissues were collected and ground in liquid nitrogen before resuspension in 5 ml of extraction buffer (20 mM Tris–HCl at pH 7.5, 150 mM NaCl, 5mM MgCl2, 1 mM DTT, 0.5% NP40, proteinase inhibitor cocktail; Sigma). The extract was then precleared by incubation with 50 ul of Protein A-agarose beads (Roche) at 4°C for 30 min. The precleared extract was incubated with 10 ul of AGO1-specific antibody for 6 hours. A volume containing 50 ul of Protein A -agarose beads (Roche) was then added to the extract before overnight incubation. Immunoprecipitates were washed three times (5 min each) in wash buffer (20 mM Tris–HCl at pH 7.5, 150 mM NaCl, 5mM MgCl2, 1 mM DTT, 0.5% Triton x-100, proteinase inhibitor cocktail; Sigma). RNA was extracted from the bead-bound EVs with TRIzol reagent (Invitrogen).

### Leaf inoculation

Tomato detached leaves were collected from 5-6 weeks old tomato plants. *B. cinerea* conidia were harvested from HA plate, where *Botrytis* had grown for 2 weeks. The conidia were adjusted

the final concentration to 10 conidia/µl and resuspended in 1% malt extract for 1 hour. Tomato leaves were inoculated with 10 µl conidia suspension. Infected leaves were incubated in a humidity box. Infected phenotypes were photographed and quantified the lesion size using the Fiji software, ImageJ version 2.1.0/1.53c (Schindelin *et al.*, 2012).

**Reverse transcriptase PCR**

CTAB-based RNA extraction method is used in this study (Bemm *et al.*, 2016). Stem-loop PCR-based reverse transcription was performed with 1 µg total RNA using SuperScript™ III Reverse Transcriptase (Thermo Fisher Scientific) with small RNA specific primers (Varkonyi-Gasic *et al.*, 2007b). Reverse transcription is performed with a thermos cycler and incubated at 16°C 30 min, followed by 60 cycles of 30°C 30 sec, 42°C 20 sec, 50°C 1 sec. Samples were in the end heated up at 85°C 15 sec then kept at 4 °C for short storage. Stem-loop PCR was performed using GoTaq G2 Polymerase (Promega) together with stem-loop universal reverse primer and sRNA-specific forward primer.

**Competing interests**

The authors declare no competing interests.

**Acknowledgments**

This work was supported by grants from the National Institutes of Health (R35GM136379), National Science Foundation (IOS 2020731), United State Department of Agriculture (2021-67013-34258) and the CIFAR 'Fungal Kingdom' fellowship to H.J..

## References


Bartel, D. P. (2009) MicroRNAs: target recognition and regulatory functions. *Cell,* **136,** 215-233.

Bemm, F., Becker, D., Larisch, C., Kreuzer, I., Escalante-Perez, M., Schulze, W. X.*, et al.* (2016) Venus flytrap carnivorous lifestyle builds on herbivore defense strategies. *Genome Research,* **26,** 812-825.

Bonath, F., Domingo-Prim, J., Tarbier, M., Friedländer, M. R. and Visa, N. (2018) Next-generation sequencing reveals two populations of damage-induced small RNAs at endogenous DNA double-strand breaks. *Nucleic Acids Res,* **46,** 11869-11882.

Buck, A. H., Coakley, G., Simbari, F., McSorley, H. J., Quintana, J. F., Le Bihan, T.*, et al.* (2014) Exosomes secreted by nematode parasites transfer small RNAs to mammalian cells and modulate innate immunity. *Nat Commun,* **5,** 5488.

Cai, Q., Qiao, L., Wang, M., He, B., Lin, F. M., Palmquist, J.*, et al.* (2018) Plants send small RNAs in extracellular vesicles to fungal pathogen to silence virulence genes. *Science,* **360,** 1126-1129.

Choquer, M., Robin, G., Le Pêcheur, P., Giraud, C., Levis, C. and Viaud, M. (2008) Ku70 or Ku80 deficiencies in the fungus Botrytis cinerea facilitate targeting of genes that are hard to knock out in a wild-type context. *FEMS Microbiol Lett,* **289,** 225-232.

Chow, F. W., Koutsovoulos, G., Ovando-Vázquez, C., Neophytou, K., Bermúdez-Barrientos, J. R., Laetsch, D. R.*, et al.* (2019) Secretion of an Argonaute protein by a parasitic nematode and the evolution of its siRNA guides. *Nucleic Acids Res,* **47,** 3594-3606.

Cui, C., Wang, Y., Liu, J., Zhao, J., Sun, P. and Wang, S. (2019) A fungal pathogen deploys a small silencing RNA that attenuates mosquito immunity and facilitates infection. *Nat Commun,* **10,** 4298.

Dunker, F., Trutzenberg, A., Rothenpieler, J. S., Kuhn, S., Pröls, R., Schreiber, T.*, et al.* (2020) Oomycete small RNAs bind to the plant RNA-induced silencing complex for virulence. *Elife,* **9**.

Feng, H., Xu, M., Liu, Y., Dong, R., Gao, X. and Huang, L. (2017) Dicer-Like Genes Are Required for H(2)O(2) and KCl Stress Responses, Pathogenicity and Small RNA Generation in Valsa mali. *Front Microbiol,* **8,** 1166.

Gandía, M., Xu, S., Font, C. and Marcos, J. F. (2016) Disruption of ku70 involved in non-homologous end-joining facilitates homologous recombination but increases temperature sensitivity in the phytopathogenic fungus Penicillium digitatum. *Fungal Biol,* **120,** 317-323.

Ji, H. M., Mao, H. Y., Li, S. J., Feng, T., Zhang, Z. Y., Cheng, L.*, et al.* (2021) Fol-milR1, a pathogenicity factor of Fusarium oxysporum, confers tomato wilt disease resistance by impairing host immune responses. *New Phytol,* **232,** 705-718.

Lee, H. C., Chang, S. S., Choudhary, S., Aalto, A. P., Maiti, M., Bamford, D. H.*, et al.* (2009) qiRNA is a new type of small interfering RNA induced by DNA damage. *Nature,* **459,** 274-277.

Leisen, T., Werner, J., Pattar, P., Safari, N., Ymeri, E., Sommer, F.*, et al.* (2022) Multiple knockout mutants reveal a high redundancy of phytotoxic compounds contributing to necrotrophic pathogenesis of Botrytis cinerea. *PLoS Pathog,* **18,** e1010367.

Lu, W. T., Hawley, B. R., Skalka, G. L., Baldock, R. A., Smith, E. M., Bader, A. S.*, et al.* (2018) Drosha drives the formation of DNA:RNA hybrids around DNA break sites to facilitate DNA repair. *Nat Commun,* **9,** 532.

Pinedo, C., Wang, C. M., Pradier, J. M., Dalmais, B., Choquer, M., Le Pêcheur, P.*, et al.* (2008) Sesquiterpene synthase from the botrydial biosynthetic gene cluster of the phytopathogen Botrytis cinerea. *ACS Chem Biol,* **3,** 791-801.

Porquier, A., Tisserant, C., Salinas, F., Glassl, C., Wange, L., Enard, W.*, et al.* (2021) Retrotransposons as pathogenicity factors of the plant pathogenic fungus Botrytis cinerea. *Genome Biol,* **22,** 225.

Qin, S., Veloso, J., Baak, M., Boogmans, B., Bosman, T., Puccetti, G.*, et al.* (2022) Molecular characterization reveals no functional evidence for naturally occurring cross-kingdom RNA interference in the early stages of Botrytis cinerea-tomato interaction. *Mol Plant Pathol*.

Ren, B., Wang, X., Duan, J. and Ma, J. (2019) Rhizobial tRNA-derived small RNAs are signal molecules regulating plant nodulation. *Science,* **365,** 919-922.

Sahr, T., Escoll, P., Rusniok, C., Bui, S., Pehau-Arnaudet, G., Lavieu, G.*, et al.* (2022) Translocated Legionella pneumophila small RNAs mimic eukaryotic microRNAs targeting the host immune response. *Nat Commun,* **13,** 762.

Schindelin, J., Arganda-Carreras, I., Frise, E., Kaynig, V., Longair, M., Pietzsch, T.*, et al.* (2012) Fiji: an open-source platform for biological-image analysis. *Nature methods,* **9,** 676-682.

Shahid, S., Kim, G., Johnson, N. R., Wafula, E., Wang, F., Coruh, C.*, et al.* (2018) MicroRNAs from the parasitic plant Cuscuta campestris target host messenger RNAs. *Nature,* **553,** 82-85.

Tang, K. F. and Ren, H. (2012) The role of dicer in DNA damage repair. *Int J Mol Sci,* **13,** 16769-16778.

Varkonyi-Gasic, E., Wu, R., Wood, M., Walton, E. F. and Hellens, R. P. (2007a) Protocol: a highly sensitive RT-PCR method for detection and quantification of microRNAs. *Plant Methods,* **3,** 12.

Varkonyi-Gasic, E., Wu, R., Wood, M., Walton, E. F. and Hellens, R. P. (2007b) Protocol: a highly sensitive RT-PCR method for detection and quantification of microRNAs. *Plant methods,* **3,** 1-12.

Wang, M., Weiberg, A., Lin, F. M., Thomma, B. P., Huang, H. D. and Jin, H. (2016) Bidirectional cross-kingdom RNAi and fungal uptake of external RNAs confer plant protection. *Nat Plants,* **2,** 16151.

Wang, Q., An, B., Hou, X., Guo, Y., Luo, H. and He, C. (2017) Dicer-like Proteins Regulate the Growth, Conidiation, and Pathogenicity of Colletotrichum gloeosporioides from Hevea brasiliensis. *Front Microbiol,* **8,** 2621.

Weiberg, A., Wang, M., Bellinger, M. and Jin, H. (2014) Small RNAs: a new paradigm in plant-microbe interactions. *Annu Rev Phytopathol,* **52,** 495-516.

Weiberg, A., Wang, M., Lin, F. M., Zhao, H., Zhang, Z., Kaloshian, I.*, et al.* (2013) Fungal small RNAs suppress plant immunity by hijacking host RNA interference pathways. *Science,* **342,** 118-123.

Werner, B. T., Koch, A., Šečić, E., Engelhardt, J., Jelonek, L., Steinbrenner, J.*, et al.* (2021) Fusarium graminearum DICER-like-dependent sRNAs are required for the suppression of host immune genes and full virulence. *PLoS One,* **16,** e0252365.

Wilczynska, A. and Bushell, M. (2015) The complexity of miRNA-mediated repression. *Cell Death Differ,* **22,** 22-33.

Wong-Bajracharya, J., Singan, V. R., Monti, R., Plett, K. L., Ng, V., Grigoriev, I. V.*, et al.* (2022) The ectomycorrhizal fungus Pisolithus microcarpus encodes a microRNA

involved in cross-kingdom gene silencing during symbiosis. *Proc Natl Acad Sci U S A,* **119**.

Yan, J., Gu, Y., Jia, X., Kang, W., Pan, S., Tang, X.*, et al.* (2012) Effective small RNA destruction by the expression of a short tandem target mimic in Arabidopsis. *Plant Cell,* **24,** 415-427.

Yin, C., Zhu, H., Jiang, Y., Shan, Y. and Gong, L. (2020) Silencing Dicer-Like Genes Reduces Virulence and sRNA Generation in Penicillium italicum, the Cause of Citrus Blue Mold. *Cells,* **9**.

Zhang, B. S., Li, Y. C., Guo, H. S. and Zhao, J. H. (2022) Verticillium dahliae Secretes Small RNA to Target Host MIR157d and Retard Plant Floral Transition During Infection. *Front Plant Sci,* **13,** 847086.

**Table 1: Dataset IDs of sRNA libraries, and some of them were deposited into NCBI. NA: Not available.**

| Description | Samples in Qin *et al*. (2022) | Read depth | Data deposited to NCBI |
|---|---|---|---|
| *B. cinerea*-inoculated tomato12 hpi | I12As | 76.4 M | SRR8074941 |
| | I12Bs | 80.4 M | SRR8074948 |
| | I12Cs | 78.8 M | SRR8074949 |
| *B. cinerea*-inoculated tomato 16 hpi | I16As | 82.7 M | SRR8074939 |
| | I16Bs | 32.8 M | SRR8074938 |
| | I16Cs | 31.4 M | SRR8074937 |
| *B. cinerea*-inoculated tomato 24 hpi | I24Bs | 60.3 M | SRR8074936 |
| | I24Ds | 89.0 M | SRR8074935 |
| mock-inoculated tomato 12 hpi | M12As | 27.4 M | SRR8074934 |
| | M12Bs | 15.2 M | NA |
| mock-inoculated tomato 16 hpi | M16As | 38.8 M | SRR8074933 |
| | M16Bs | 21.1 M | NA |
| mock-inoculated tomato 24 hpi | M24As | 25.4 M | SRR8074932 |
| | M24Ds | 18.7 M | NA |
| *B. cinerea* liquid culture 16 hpi | B16As | 56.7 M | SRR8074931 |
| | B16Bs | 22.6 M | SRR8074930 |
| *ku70* knockout mutant | *ku70*-1s | 18.4 M | NA |
| | *ku70*-2s | 23.8 M | NA |
| | *ku70*-3s | 15.3 M | NA |
| Δ*bcdcl1*/Δ*bcdcl2* mutant in *ku70* | *dcl1dcl2*-1-26s | 18.2 M | NA |
| | *dcl1dcl2*-1-29s | 22.6 M | NA |
| | *dcl1dcl2*-1-30s | 17.2 M | NA |

**Table 2: Dataset IDs of mRNA libraries, and some of them were deposited into NCBI. NA: Not available.**

| Description | Samples in Qin *et al*. (2022) | Read depth | Data deposited to NCBI |
|---|---|---|---|
| *B. cinerea*-inoculated tomato 12 hpi | I12Am | 72.2 M | SRR8074958 |
| | I12Bm | 69.0 M | SRR8074959 |
| | I12Cm | 24.9 M | SRR8074956 |
| *B. cinerea*-inoculated tomato 16 hpi | I16Am | 69.2 M | SRR8074957 |
| | I16Bm | 71.9 M | SRR8074954 |
| | I16Cm | 25.8 M | SRR8074955 |
| *B. cinerea*-inoculated tomato 24 hpi | I24Bm | 70.1 M | SRR8074952 |
| | I24Cm | 26.1 M | SRR8074950 |
| | I24Dm | 74.4 M | SRR8074953 |
| mock-inoculated tomato 12 hpi | M12Am | 25.3 M | SRR8074951 |
| | M12Bm | 26.7 M | SRR8074946 |
| mock-inoculated tomato 16 hpi | M16Am | 23.5 M | SRR8074947 |
| | M16Bm | 24.5 M | SRR8074944 |
| | M16Dm | 22.9 M | NA |
| mock-inoculated tomato 24 hpi | M24Am | 18.3 M | SRR8074945 |
| | M24Dm | 4.2 M | SRR8074942 |
| *B. cinerea* liquid culture 16 hpi | B16Am | 22.1 M | SRR8074943 |

| | | | |
|---|---|---|---|
| | B16Bm | 22.2 M | SRR8074940 |
| *ku70* knockout mutant | *ku70*-1m | 22.4 M | NA |
| | *ku70*-2m | 22.3 M | NA |
| | *ku70*-3m | 23.0 M | NA |
| Δ*bcdcl1*/Δ*bcdcl2* mutant in *ku70* | *dcl1dcl2*-1-26m | 23.8 M | NA |
| | *dcl1dcl2*-1-29m | 24.4 M | NA |
| | *dcl1dcl2*-1-30m | 22.3 M | NA |

# Figure 1

A

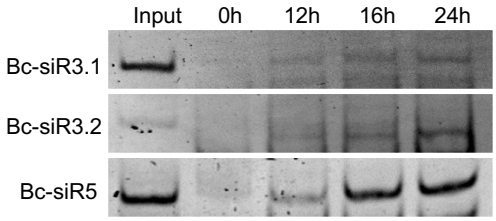


B

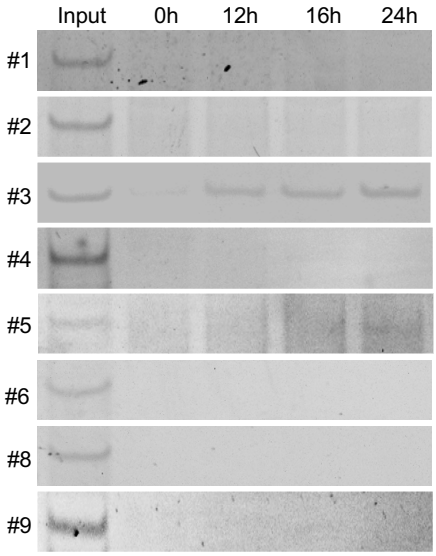


| ID | sequence | map | loci | sRNAseq* (WT/d12) |
|---|---|---|---|---|
| #1 | TCTTCTCCTCCGACTGGGATGT | RT | 4 | Y/N |
| #2 | TGATGTGGAGCGGGTTTCCAAG | Exon (S) | 1 | Y/N |
| #3 | TATCCATGGGTTCAGTATCT | RT, exon (AS) | 5 | Y/N |
| #4 | TCATAATTTAATTCGGCTGGTG | RT | 1 | Y/N |
| #5 | CATTCTTACATATTCTGATT | snoRNA | 1 | Y/Y |
| #6 | TGGTAATTCTAGAGCTAATA | rRNA | 1 | Y/Y |
| #7 | GTAGTTGGTTATCACATTCCC | tRNA | 1 | Y/Y |
| #8 | TTTTCTTGTTCTCTTCTTTTT | RT | 2 | Y/N |
| #9 | ATAATGAAGAACAAACAAACC | UTR | 1 | Y/Y |

* Wang et al 2016, Y (Yes), N (No); S (sense), AS (antisense)

C

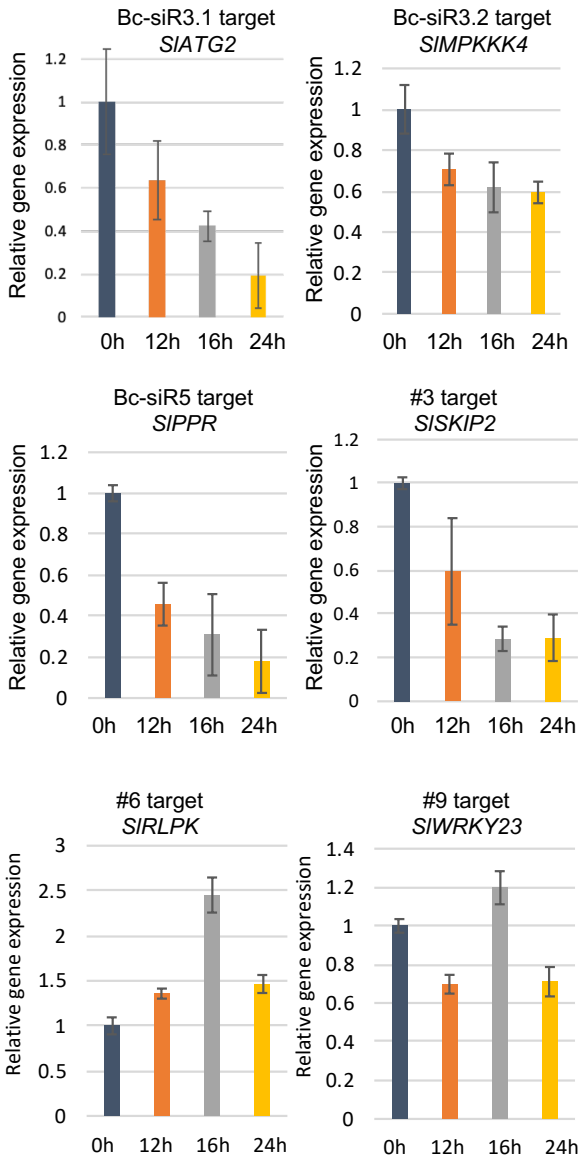

Figure 2

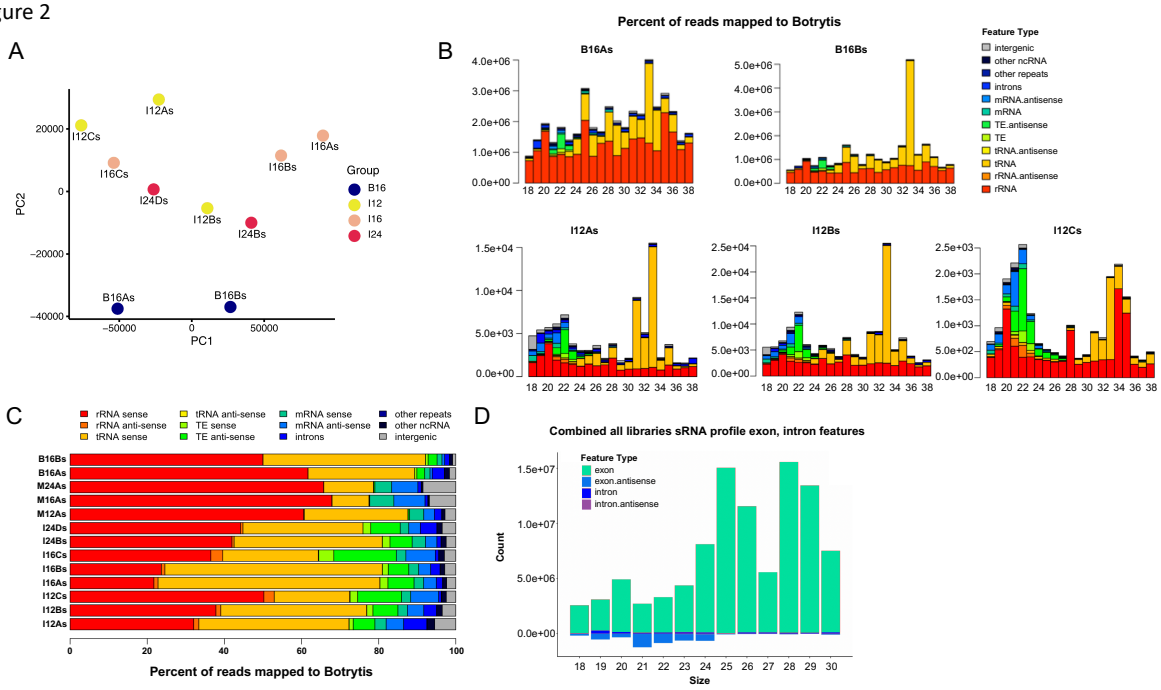
A
I12As
I12Cs
I16As
I16Cs
I16Bs
I24Ds
I12Bs
I24Bs
B16As
B16Bs
PC2
PC1
Group
B16
I12
I16
I24
B
Percent of reads mapped to Botrytis
B16As
B16Bs
I12As
I12Bs
I12Cs
Feature Type
intergenic
other ncRNA
other repeats
introns
mRNA.antisense
mRNA
TE.antisense
TE
tRNA.antisense
tRNA
rRNA.antisense
rRNA
C
rRNA sense
rRNA anti-sense
tRNA sense
tRNA anti-sense
TE sense
TE anti-sense
mRNA sense
mRNA anti-sense
introns
other repeats
other ncRNA
intergenic
B16Bs
B16As
M24As
M16As
M12As
I24Ds
I24Bs
I16Cs
I16Bs
I16As
I12Cs
I12Bs
I12As
Percent of reads mapped to Botrytis
D
Combined all libraries sRNA profile exon, intron features
Feature Type
exon
exon.antisense
intron
intron.antisense
Count
Size

Figure 3

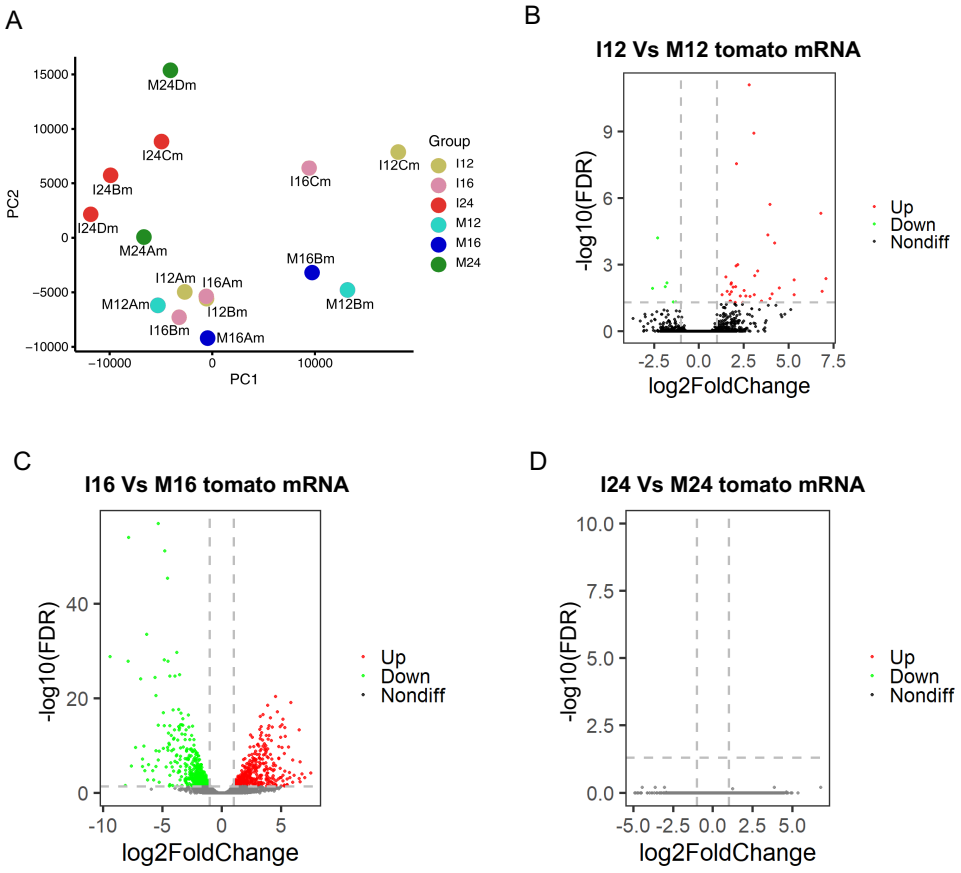
A
PC2
PC1
15000
10000
5000
0
−5000
−10000
−10000
0
10000
M24Dm
I24Cm
I24Bm
I24Dm
M24Am
I16Cm
I12Cm
M16Bm
I12Am
I16Am
M12Am
I12Bm
I16Bm
M16Am
M12Bm
Group
I12
I16
I24
M12
M16
M24
B
I12 Vs M12 tomato mRNA
-log10(FDR)
log2FoldChange
Up
Down
Nondiff
C
I16 Vs M16 tomato mRNA
-log10(FDR)
log2FoldChange
Up
Down
Nondiff
D
I24 Vs M24 tomato mRNA
-log10(FDR)
log2FoldChange
Up
Down
Nondiff

Figure 4

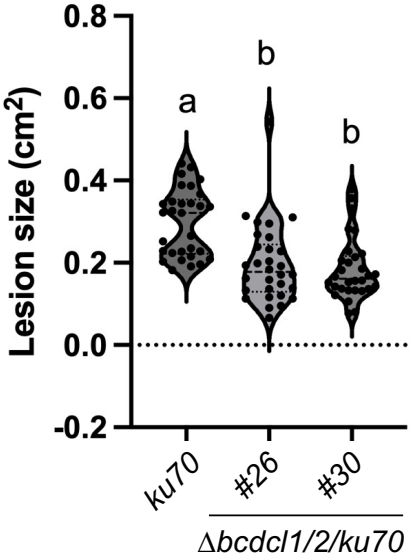
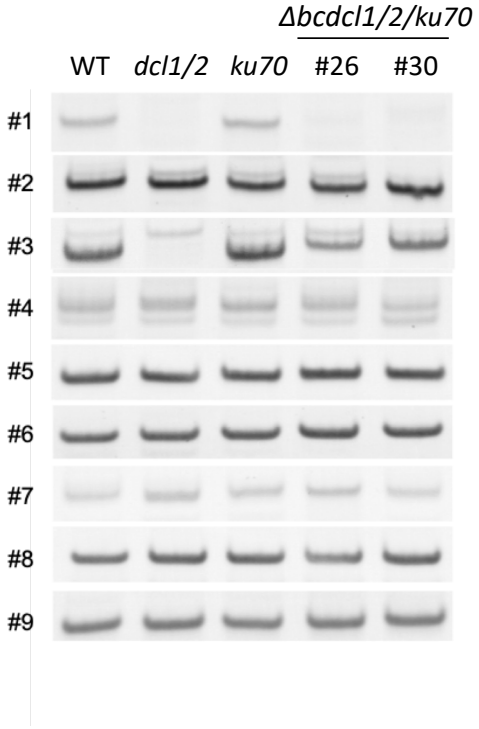
Figure 5